ADVANCED FUNCTIONAL MATERIALS
www.afm-journal.de

# Nanoliter Liquid Packaging in a Bioresorbable Microsystem by Additive Manufacturing and its Application as a Controlled Drug Delivery Device

*Jongeon Park, Arnaud Bertsch, Cristina Martin-Olmos, and Juergen Brugger**

**Precise packaging of nanoliter amounts of liquid in a microsystem is important for many biomedical applications. However, existing liquid encapsulation technologies have limitations in terms of liquid waste, evaporation, trapped bubbles, and liquid degradation. In this study, multiple additive manufacturing techniques for nanoliter liquid packaging in bioresorbable microsystems is used. Two-photon photolithography is used for bioresorbable reservoir fabrication, while inkjet printing (IJP) is used for precise nanoliter liquid packaging. Dual IJP allows for micro-reservoirs to be filled with precise amounts of drug solution and subsequently and rapidly sealed with a layer of lipids mixed with $Fe_3O_4$ nanoparticles. Combining these two printing techniques can overcome the previous limitations of liquid encapsulation technologies. To demonstrate the relevance of this technique, a wirelessly activated, bioresorbable multi-reservoir microcapsule that can be used for controlled drug delivery is presented. The microcapsules and their content are shown to be stable during fabrication, storage, and operation. Multiple cargo release events are triggered independently by the local melting of the sealing layer, resulting from magnetically induced $Fe_3O_4$ nanoparticle heating. The operation of the capsule is demonstrated in tissue phantoms and in vitro cell cultures.**

## 1. Introduction

Packaging nanoliter (nL) to microliter (µL) volumes of liquid in microsystems is significant for biomedical applications. Particularly for lab-on-chip,[1] microanalytical systems,[2] and drug delivery systems,[3] providing reservoirs filled with reactants or drugs on microsystems simplifies these systems by minimizing their interface with external components and protecting the cargo. However precisely packaging nL volumes of liquid inside sealed micro-reservoirs is more challenging than it may seem. In some reported cases, evaporation of the liquid during the fabrication process is an issue that prevents the filling of the reservoirs with a precisely defined amount of liquid.[4] Several techniques have been reported to minimize the loss of nL-volume liquid during packaging. "In-liquid" sealing approaches, which are based on the alignment and bonding of the micro-reservoir and sealing layer while immersed in a large volume of the liquid that is supposed to be packaged in the reservoir, have been developed.[5] Okayama et al. developed an in-liquid bonding technique that enables the sealing of silicon cavities filled with aqueous and glycerin-based liquids using a PDMS membrane and UV adhesive. However, direct UV irradiation of the encapsulated liquid is not suitable for biomedical applications as many drugs and biomolecules degrade under such conditions.[6] Vastesson et al.[5b] presented an in-liquid bonding method based on the bonding between gold films and reservoirs made of off-stoichiometry thiol-ene polymer and encapsulated nL to µL amounts of aqueous drug solution. Although in-liquid sealing can be used successfully to package a precise amount of liquid without loss during fabrication, a large amount of liquid is wasted during fabrication, which is not appropriate when encapsulating expensive materials.

To minimize liquid waste, the "fill, and seal" approach in which the reservoir is manually filled, then sealed with a metal or polymer layer can be used.[7] Matsumoto et al.[7a] encapsulated nL amounts of liquid inside silicon cavities coated with parylene by bonding it at 200 °C. However, this method proved to be unreliable for packaging precise amounts of liquid in each reservoir and is not appropriate for liquids having a low

J. Park, A. Bertsch, J. Brugger
Microsystems Laboratory (EPFL-STI-IEM-LMIS1) Ecole Polytechnique Fédérale de Lausanne (EPFL)
Lausanne 1015, Switzerland
E-mail: juergen.brugger@epfl.ch
C. Martin-Olmos
Center for Advanced Surface Analysis
Institute of Earth Sciences
University of Lausanne (UNIL)
Lausanne 1015, Switzerland
C. Martin-Olmos
School of Architecture
Civil and Environmental Engineering
EPFL
Lausanne 1015, Switzerland

The ORCID identification number(s) for the author(s) of this article can be found under https://doi.org/10.1002/adfm.202302385



**DOI: 10.1002/adfm.202302385**

boiling point and for encapsulating temperature-sensitive cargo. Another drawback of the "fill and seal" approach is that it is very difficult to completely fill a reservoir with liquid due to the evaporation of the liquid during the time gap between filling and sealing that is caused by the alignment and bonding of the sealing layer.[7b] Furthermore, air bubbles are generally trapped in sealed reservoirs, which can interfere with the operation of the liquids on-chip.

Liquid packaging can be improved by using a self-assembled polymer membrane to form a sealing layer directly over the liquid surface, rather than bonding the sealing layer. This approach can mitigate issues with liquid evaporation and prevent the entrapment of air bubbles during fabrication, as it does not require alignment or bonding processes. Recently, Coppola et al.[8] developed a rapid liquid packaging method based on poly lactic-co-glycolic acid (PLGA) film formation on a water interface, which exploits the Marangoni spreading of PLGA dissolved in dimethyl carbonate (DMC) above water and subsequently followed by the diffusion of the organic solvent into the aqueous phase. The organic solvent extraction into the aqueous phase, which allows the formation of the PLGA films has the disadvantage of being toxic to cells. Additionally mixing an organic solvent with the aqueous phase may have an adverse effect on drugs or biological cargo, which makes this liquid encapsulation method inappropriate for most biomedical applications.

In summary, the major drawbacks of liquid packaging techniques presented so far are their compatibility with cargo, liquid evaporation, and liquid waste. Furthermore, previous studies have not considered cargo alteration or liquid loss during reservoir sealing, as well as the passive and active release of packaged cargo. However, these considerations are important when applying liquid packaging in a biomedical context, such as drug release applications.[9]

We propose using dual inkjet printing (IJP) as a method for precisely packaging nL volumes of liquid in microcapsules with minimal liquid loss, minimal effect on the cargo, and minimal cargo waste. To create a small multi-reservoir capsule that could pass through a syringe, we used two-photon polymerization (TPP) with a biocompatible and bioreorbable polymer based on polyethylene glycol diacrylate (PEGDA).[10] We filled the capsule using IJP with drugs that had different pharmacokinetics, hydrophilic, and lipophilic properties. We precisely dispensed a controlled volume of drugs into each reservoir, which was then sealed by IJP with a layer of molten lipids mixed with magnetic nanoparticles (MNP) that was subsequently solidified. The IJP of the lipid MNP mixture sealing layer is performed within a few seconds after the first IJP of the drugs. This minimizes liquid evaporation and cargo degradation during fabrication while also enabling the on-demand opening of the solidified sealing layer through alternating magnetic field (AMF)-triggered heating. We investigated the effect of fabrication, storage, and in vitro operation on the packaged cargo, including quantitatively examining liquid loss during fabrication and storage. We also looked at the physical and chemical alteration of the cargo and capsule during fabrication, storage, and in vitro operation over a prolonged period, as well as the cargo release from the capsule. We performed controlled drug release from the fabricated device in vitro using cell cultures and tissue phantoms to demonstrate the feasibility of the capsule obtained by the proposed liquid packaging technology as a drug delivery system.

## 2. Results

### 2.1. Nano-Liter Liquid Packaging in a Microcapsule by Dual IJP

A bioresorbable micro-reservoir was fabricated by TPP techniques using a PEGDA-based photoresist (**Figure 1**A). It has a square footprint, with side lengths of 800 μm and a total height of 500 μm, which makes it small enough for injection through a 17-gauge syringe. Its lower part is composed of 9 identical independent containers of cylindrical shape, each having a volume of 5.6 nL, to be filled with the drug solutions. On top of each reservoir, a 200 μm × 200 μm square cavity of different heights (170, 120, and 70 μm) is defined to be filled with the sealing layer inks.

A precise filling method was used to fill each reservoir in the capsule with ≈5.6 nL of drug solution using IJP technology. The drug solution was dispensed in 50 droplets, each having a volume of ≈113 pL, as shown in Figure 1B. The hydrophilic and lipophilic drugs, including 5-fluorouracil (5-FU), docetaxel (DTX), doxorubicin hydrochloride (DOX), and curcumin (CUR), were printed using dimethyl sulfoxide (DMSO) aqueous solutions as a solvent. The stability of these drugs in solution was appropriate for liquid drug delivery as they are stable at −20 °C and slowly degrade ≈37 °C. [11] DMSO, an amphiphilic solvent, was used as a co-solvent to dissolve a mixture of hydrophilic and lipophilic drugs. It is classified as a class 3 solvent by the FDA and is considered safe for use inside the body in small amounts (less than 50 mg per day).[12] The composition of the drug solutions used in our study is presented in **Table 1**, where each drug was chosen as its saturated concentration at different DMSO concentrations to achieve maximum drug loading. To visualize the solution encapsulation, 1 mg $mL^{-1}$ of Methylene blue (MB) was added to the solution. The viscosity of the solutions was suitable for the IJP process to take place at room temperature, which did not affect the drug stability in any way.

Figure 1C, shows how IJP was utilized to dispense the sealing layer for each container that had been previously filled with the drug solution. In this process, different print heads in the same inkjet printer were utilized for both filling the reservoirs with the drug solution and then closing them by printing the sealing material. This method, which we have termed "dual IJP" in this paper allowed for a rapid switch, less than 5 s between dispensing the drug solution and the sealing layer. Since the amount of liquid evaporation is proportional to the time between dispensing of liquid cargo and the sealing layer, this method of operation minimizes liquid losses due to evaporation and allows for precise control of the volumes encapsulated. A detailed demonstration of the entire printing process of filling and sealing of the drug solution by dual IJP is shown in Video S1 (Supporting Information).

The sealing material used in this study is a lipid mixture consisting of mono-, di-, and triglycerides esters of fatty acids with a low hydroxide ratio (Suppocire CM), which includes 0.5 wt.% of lecithin and 8 wt.% of lipid-coated $Fe_3O_4$ nanoparticles as MNPs. The homogenous distribution of nanoparticles

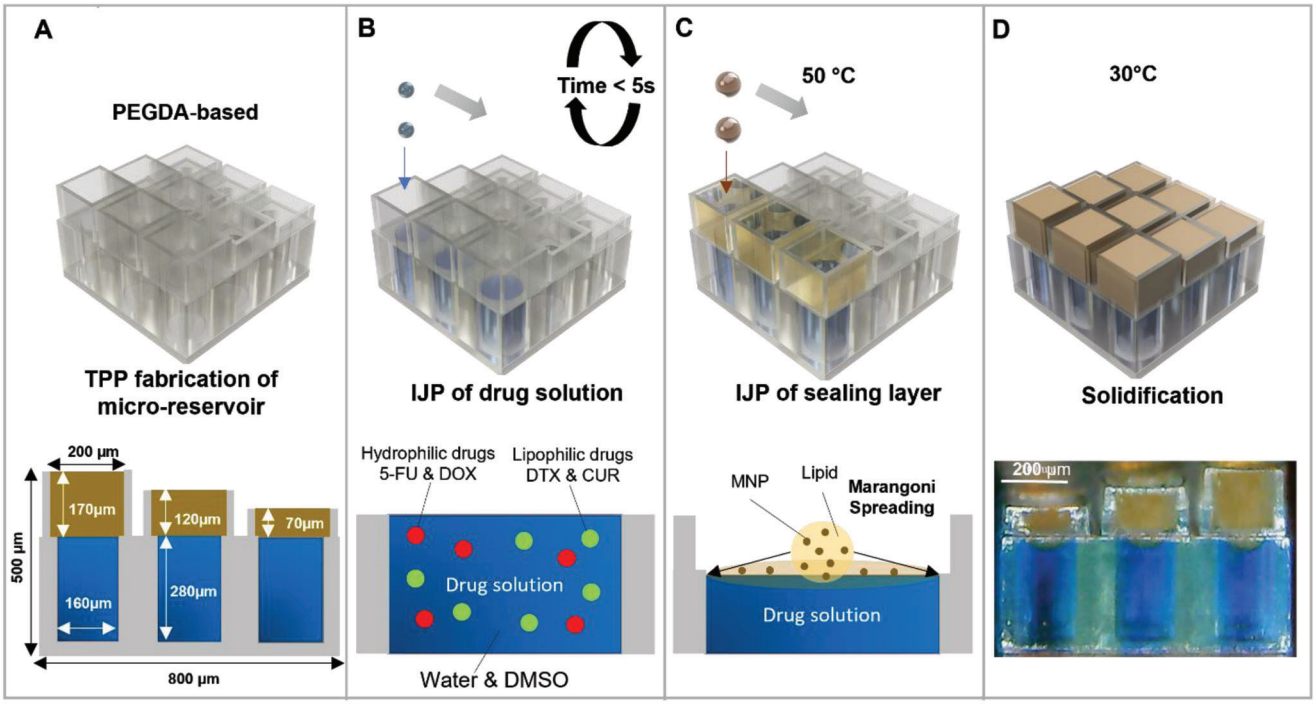


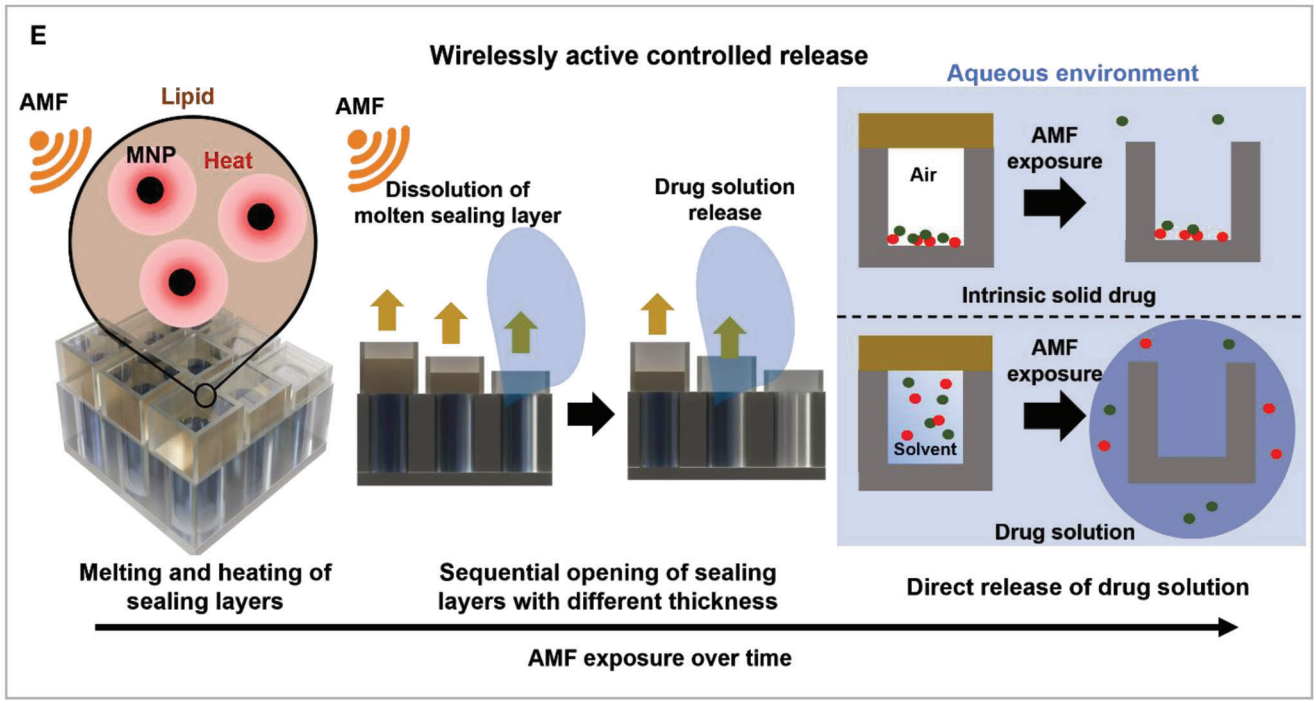


**Figure 1.** Nanoliter liquid packaging in micro-reservoir by IJP. Schematics of the fabrication process: A) Top: TPP fabrication of PEGDA-based micro-reservoir. Bottom: Design and dimension of drug solution packaged capsule composed with sealing layer, drug solution, and PEGDA reservoir. B) IJP of solution of drugs with multiple pharmacokinetics dissolved in DMSO-aqueous solvent. C) Top: IJP of the molten lipid-MNP mixture after IJP of drug solutions with a time gap of less than 5 s (dual IJP). Bottom: Marangoni spreading molten lipid-MNP above the drug solution. D) Top: Solidification of the lipid sealing layer at 30 °C for 6 h. Bottom: Optical image of the final capsule. E) Wirelessly active controlled release feature of the capsule: 1. Heating and melting of sealing layers by AMF heating of incorporated MNP in the sealing layer 2. Sequential opening of sealing layers with different thicknesses by their dissolution time gap 3. Direct release of drug solution that enables simultaneous delivery of multiple drugs with different pharmacokinetics.

**Table 1.** Composition of all solutions used in this study.

| Solution n° | DMSO [%] | Water [%] | 5-FU [mg mL$^{-1}$] | DTX [mg mL$^{-1}$] | DOX [mg mL$^{-1}$] | CUR [mg mL$^{-1}$] |
|---|---|---|---|---|---|---|
| 1 | 70 | 30 | 50 | 10 | 0 | 0 |
| 2 | 30 | 70 | 30 | 3 | 0 | 0 |
| 3 | 70 | 30 | 0 | 0 | 50 | 10 |
| 4 | 30 | 70 | 0 | 0 | 30 | 3 |
| 5 | 70 | 30 | 50 | 0 | 0 | 0 |
| 6 | 70 | 30 | 0 | 10 | 0 | 0 |
| 7 | 30 | 70 | 30 | 0 | 0 | 0 |
| 8 | 30 | 70 | 0 | 3 | 0 | 0 |

in the molten lipid-MNP mixture without aggregation has been confirmed by direct light scattering (DLS) measurement (Figure S1A, Supporting Information). The lipid-MNP mixture has a melting temperature of 39 °C; therefore, the print head is heated to 50 °C during the IJP process to lower the viscosity of the molten lipid-MNP mixture (Figure S1B, Supporting Information). When heated to 50 °C, the lipid mixture melts and exhibits a lower density (0.86 g mL$^{-1}$) and lower surface tension than water, allowing it to spread out evenly above the aqueous drug solution by the Marangoni effect. The estimated temperature of the molten lipid droplet when it lands on the liquid surface is 49.9 °C, indicating that the lipid droplet remains in a molten state when it lands on the liquid surface (Supporting text 1). Once cooled down, the lipid mixture reverts to its solid form and forms a tight seal for each reservoir. The lipid mixture is insoluble in water in its solid form and has very low solubility in water in its molten state. The effect of DMSO on the lipid mixture was also investigated. Additionally, the lipid layer is biocompatible and enzymatically degrades in the human body,[13] making it an attractive material for liquid packaging in biomedical applications.

Finally, the microcapsule with the encapsulated liquid cargo was solidified at 30 °C for 6 h (Figure 1D). After solidification, the capsule was stored at −20 °C to minimize the vapor pressure and vapor permeation through the capsule and to prevent the degradation of the encapsulated drugs.[11] Figure 1D displays an optical camera image of the final liquid encapsulated capsule, with the brown upper layer representing the lipid-MNP sealing layer and the blue liquid below indicating the drug solution. Additional SEM and cryo-SEM images of the resulting capsule are presented in Figure S2 (Supporting Information).

The $Fe_3O_4$ nanoparticles mixed with the lipids, exhibit a soft-magnetic behavior (Figure S1C, Supporting Information). This means that the magnetic nanoparticles present in the sealing layer can be heated using an AMF, inducing the melting of the sealing layer and the release of the corresponding reservoir content. Using an AMF for different time scales allows for the sequential opening of the various reservoirs in one capsule, depending on the thickness of the sealing layer that closes them. The thinner layer will open first, and the thickest one will open last, resulting in the possibility to trigger the release of drugs independently from each reservoir (Figure 1E). IJP allows for the precise dispensing of the required volume of the sealing layer by controlling the number of droplets, thus differentiating the thickness of the sealing layer. Therefore, multiple drug release events can be triggered at chosen points in time, or the simultaneous release of multiple drugs contained in different reservoirs can be performed. This allows for unprecedented control over the pharmacokinetic effects during drug administration.

### 2.2. Sealing Layer Characterization

In the initial version of the sealing material, which did not contain lecithin in the lipid mixture, the drug solution packaged in the capsule leaked out (Figure S3, Supporting Information). To address this issue, lecithin was added as a surfactant in the sealing layer between materials with different surface tensions: polymer surface (reservoir) and lipid (sealing layer). The addition of a moderate amount of lecithin in the sealing layer significantly reduced drug leakage. The relationship between drug leakage and lecithin concentration is presented in Figure S3 (Supporting Information). On a cross-sectioned Cryo-SEM image of the capsule without lecithin in the sealing layer, a gap between the polymer surface and the lipid sealing layer was observed (**Figure 2**A). In contrast, the sealing layer with lecithin was tightly attached to the polymer surface without gaps or defects (Figure 2B), unlike the sealing layer without lecithin.

Lipids may be crystallized into different polymorphs during cooling,[14] which can affect sealing properties and cargo release kinetics. Hence, it is important to control the physical state of the solidified lipids for the consistent quality of the capsule. We tested two different methods of solidifications, either by keeping them at 30 °C for 6 h (Method 1) or by freezing the capsules at −20 °C for a few seconds (Method 2). Solidification of the sealing layer above its glass transition temperature (Method 1) enables the transformation of unstable lipid polymorphs into the most stable crystalline form. Differential scanning calorimetry (DSC) results of a solidified lipid membrane prepared by this process showed one melting peak (Figure S1D, Supporting Information), which indicates that a solidified lipid membrane exists in one stable crystalline state.

There was a leakage of the encapsulated drug solution in the capsule prepared by Method 2, whereas the capsule prepared by Method 1 showed tight sealing without leakage (Figure S3, Supporting Information). The PEGDA-based polymer surface of the capsule was analyzed by X-ray photoelectron spectroscopy (XPS) after the removal of the solidified sealing layer in both cases. The

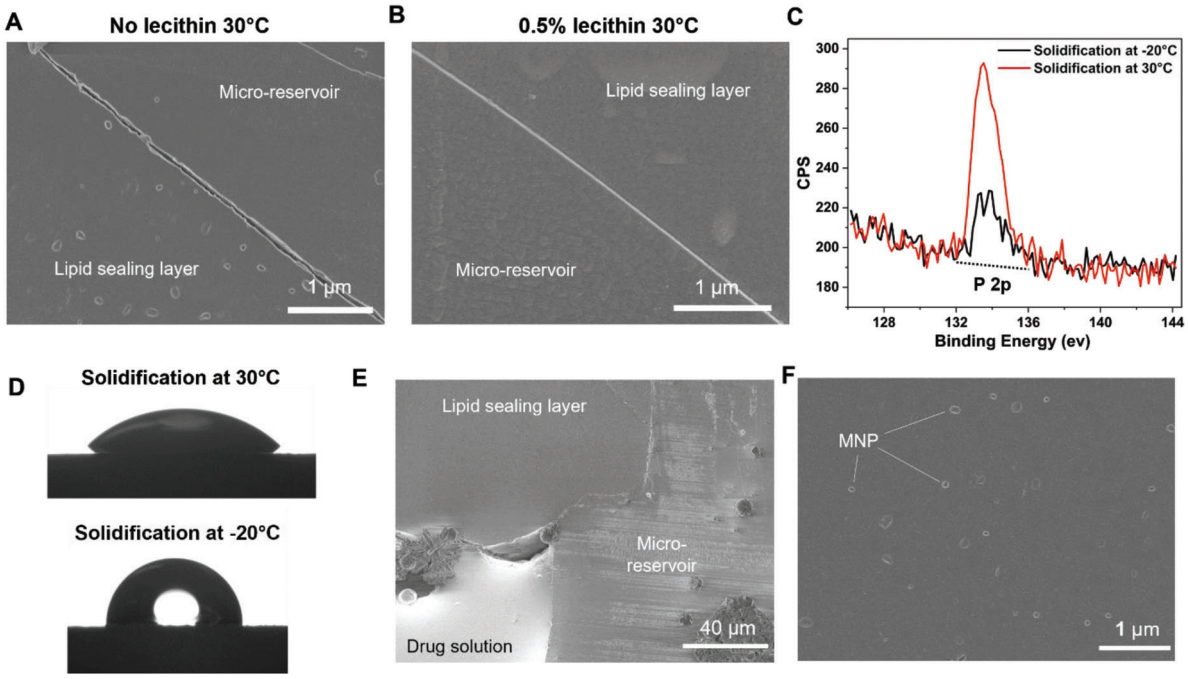


**Figure 2.** Sealing layer characterization. A) Cryo-SEM image of the interface between lipid sealing layer with no lecithin and micro-reservoir and B) interface between lipid sealing layer with 0.5% lecithin (cross-sectioned view) C) XPS result of PEGDA-based material surface that detached from lipid sealing layer after solidified at −20 and 30 °C. D) Contact angle of the PEGDA-based material surface measured 10 s after the waterdrop cast. Cryo-SEM image of the cross-section of the capsule with the sealing layer of 0.5% lecithin solidified at 30 °C for 6 h: E) Interface of lipid sealing layer, drug solution, and micro-reservoir. F) Magnified image of lipid sealing layer (the bright dots are MNPs).

XPS results exhibit a much larger 2p peak of Phosphorous for the Method 1 sample (Figure 2C), indicating that a larger amount of lecithin is present on the surface (lecithin is the only molecule involved that contains phosphorous). The contact angle of water on the same samples measured after 10 s was 38.8° and 90.5° in Method 1 and Method 2 samples, respectively (Figure 2D). Again, the presence of a larger amount of lecithin on the surface of the polymer in Method 1 can explain this drop in contact angle, with lecithin acting as a surfactant.

A cross-section of the drug solution-filled capsule obtained by Method 1 was observed by cryo-SEM. Figure 2E shows the interface between the wall of the micro-reservoir, drug solution, and sealing layer, which indicates that the drug solution is structurally isolated by the sealing layer. A high-magnification image of the sealing layer (Figure 2F) shows that it has no defects or pores and that the MNPs are homogeneously distributed and without agglomeration. The top view SEM image of the capsule shows that the upper sealing layer part that contacts with the outside environment is tightly attached to the reservoir surface without a gap (Figure S2D, Supporting Information). All these results indicate that lecithin acting as a surfactant between the micro-reservoir surface and sealing layer is a significant factor for effective sealing.

### 2.3. Liquid Loss from the Capsule During Fabrication, and Storage

**Figure 3**A displays the Thermogravimetric analysis (TGA) of a capsule containing a solution of 30% DMSO in water (Solution 2), measured immediately after fabrication and after 30 days of storage at −20 °C. Water and DMSO evaporate at 100 and 180 °C respectively, the PEGDA-based polymers decompose after 250 °C, and lipids start to decompose at 300 °C, leaving only the MNPs at a temperature higher than 500 °C. To determine the amount of liquid present in the capsule, the remaining mass after 700 °C was subtracted from the mass after the 180 °C plateau. This value was then compared to the mass calculated by multiplying the number of printed droplets by the volume of a single droplet and the density of the packaged liquid. The TGA measurement showed a 3.8% difference (52 ng) from the calculated value (54 ng), which can be attributed to liquid loss during the capsule fabrication process. To minimize this loss, inkjet print heads can be switched faster in dual IJP, or the humidity or temperature of the printing environment can be adjusted for a lower evaporation rate.

The ability of the capsule to retain its contents with minimal evaporation is crucial in determining its expiration time and distribution. After 30 days of storage at −20 °C, the remaining liquid in the capsule was 50 ng, which corresponds to a 4% difference from the calculated initial value. These results suggest that there was no significant solvent loss during the storage of the sample.

### 2.4. Characterization of the Chemical Degradation of Drugs During Fabrication, Storage, and In Vitro Operation

Liquid chromatography-mass spectrometry (LC-MS) was performed on Solution 1 to evaluate if the dissolved drugs undergo chemical degradation during storage, implantation, and

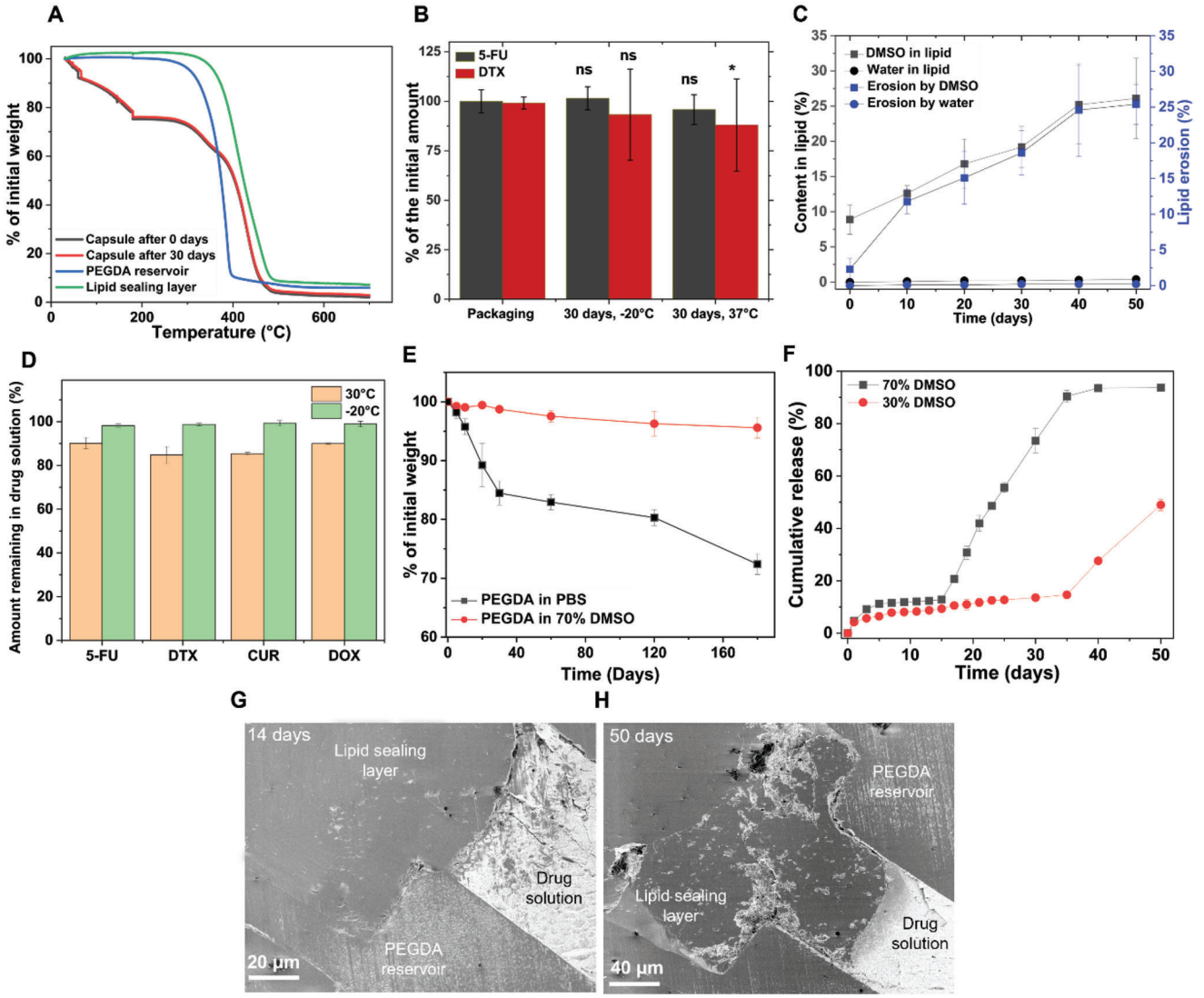


**Figure 3.** Characterization of physical and chemical alteration of packaged drug and capsule components during fabrication, storage, and in vitro operation. A) Liquid loss from the capsule: TGA analysis results of freshly fabricated device (Device after 0 days), device stored at −20 °C for 30 days (Device after 30 days), PEGDA-based micro-reservoir, and lipid sealing layer. B) Degradation of drug: % ratio of remaining 5-Fu and DTX amount with the initial state of the drug solution incubated at 37 °C (in vitro operation), and −20 °C (storage) for 30 days and drug solution after the liquid packaging process. (*$p < 0.05$; ns, $p > 0.05$; $n = 3$) C) Alteration of lipid sealing layer during in vitro operation: Amount of water and DMSO intake in the lipid membrane and amount of lipid erosion placed at 37 °C. ($n = 5$) D) Amount of drug remaining in drug solution after liquid packaging process under two different solidification temperatures (at 30 and −20 °C) % of initial drug concentration ($n = 3$) E) Alteration of the micro-reservoir during in vitro operation: Degradation amount of TPP-fabricated PEGDA-based cube placed in PBS and 70% DMSO solvent at 37 °C that obtained from TGA. ($n = 3$) F) DMSO concentration change during capsule in vitro operation: Cumulative DMSO permeation amount through the 70% DMSO and 30% DMSO aqueous solvent encapsulated capsule in PBS at 37 °C. ($n = 5$) Cryo-SEM image of the cross-section of the capsule after G) 14 days and H) 50 days of in vitro drug release.

fabrication. The 3 following conditions were tested: Storage condition: −20 °C for 30 days, In vitro condition: 37 °C for 30 days, and Packaging condition: 30 °C for 6 h after IJP. The area under the peak of the extracted ion chromatograms for 5-FU and DTX was divided with the ones of 5-FU and DTX in freshly prepared drug solution to obtain the relative remaining amount of drugs in each condition (Figure 3B). There was no significant degradation in any condition except for DTX stored at 37 °C for 30 days that shows a 5% degradation. This indicates that the effect of the liquid packaging process developed, and that the storage condition of a capsule does not induce cargo degradation. However, if a drug solution is implanted and kept at human body temperature for a prolonged period, it may degrade.

### 2.5. Characterization of the Capsule's Components Changes During In Vitro Operation

We evaluated the temporal evolution of DMSO and water content intake into the PEGDA-based reservoirs and sealing layer, as well

as the degradation of these materials. To prepare the sealing layer, we followed the same procedure as the liquid encapsulating process, which involved drop-casting the molten sealing layer on the liquid surface and solidifying it at 30 °C for 6 h, followed by placing it on the liquid surface at 37 °C. The sealing layer showed effective water-sealing properties, with less than 0.5% water intake and erosion over 50 days of the experiment (Figure 3C). However, DMSO intake into the sealing layer was 9% of the initial dry weight of the sealing layer (Figure 3C). The DMSO content of the sealing layer that solidified at −20 °C was less than 2% after 1 day, indicating that DMSO intake into the sealing layer was mainly caused by diffusion into the molten sealing layer during the solidification process. The DMSO content in the sealing layer continuously increased throughout the experiment, reaching 25% after 40 days and saturating from there (Figure 3C). The erosion of the lipid layer, which was measured by its change in dry weight, followed the same trend as the DMSO intake and appeared to stop after 40 days. This suggests that ≈25% of the molecules forming the lipid sealing layer were slowly removed for 40 days, while the rest maintained an efficient but slightly porous barrier against DMSO permeation. These results suggest the possibility of obtaining a much tighter seal by removing some of the molecules from the lipid mix and keeping only those present in the layer remaining after 40 days of exposure to DMSO.

As for the DMSO, there was drug molecules intake into the molten sealing layer during the fabrication process. This was measured by preparing a bigger capsule with the same components and design ratio compared with the previous microcapsule, by IJP the molten sealing layer on Solutions 1 and 3 in the same condition as for the capsule fabrication. Solidification of the sealing layer was carried out at 30 °C and −20 °C for 6 h to evaluate the effect of the solidification process on the drug migration. The amount of drug that diffused into the sealing layer during the fabrication process was evaluated by measuring the amount of drug remaining in the drug solution after the removal of the solidified lipid layer. For all four studied drugs, more than 10% of the drugs in drug solutions migrated into the sealing layer during fabrication with a 30 °C solidification process (Figure 3D). DTX and CUR intake into the sealing layer was slightly larger than 5-FU and DOX because of their higher partition coefficient. Less than 2% of drugs migrated into the sealing layer during the −20 °C solidification process, showing that drug intake was dominantly caused by drug diffusion into the molten sealing layer during the solidification process at 30 °C.

It has already been proven that PEGDA-based polymers can be slowly degraded by ester bond hydrolysis in vivo over months.[10] Their degradation products have low cytotoxicity and can be partially metabolized.[15] The degradation of the PEGDA-based polymer immersed either in water or in 70% DMSO was measured to investigate the PEGDA-based reservoir alteration under in vitro operation conditions. Cubes of 260 µm sides were fabricated by TPP and immersed in centrifuge tubes containing either 1 mL of PBS or 1 mL of 70% DMSO. The cubes were incubated at 37 °C for 180 days and their mass was measured at various time points, as presented in Figure 3E. After 180 days, the cubes placed in PBS lost 27% of their weight, whereas the ones in 70% DMSO lost 2.5% of their weight only. This indicates that the used PEGDA-based polymer is degraded by hydrolysis, but that the presence of DMSO inhibits this effect. The PEGDA-based polymer was found to have a low water swelling ratio (Figure S4, Supporting Information). Accelerated degradation of the capsule under 0.01 M NaOH solution is shown in Figure S5 (Supporting Information).

Further experiments were conducted to evaluate the permeation through the capsule of the solvents in which the drugs are dissolved: Solvent permeation may induce drug permeation or drug crystallization in the reservoir. The temporal evolution of the permeation of DMSO was evaluated through the capsules filled with 70% DMSO, and 30% DMSO. The capsules were prepared with the same design, dimensions, and procedures as the previous capsule (Figure 3F). The DMSO permeation through the PEGDA-based material was found to be negligible (Figure S6, Supporting Information), indicating that the DMSO permeation through the capsule dominantly occurs through the sealing layer. Both for 70% DMSO and 30% DMSO an initial DMSO release is observed, corresponding to the DMSO migration in the lipid layer during the sealing layer solidification. DMSO was slowly released from the capsule until day 15 and day 35 for 70% DMSO and 30% DMSO, respectively. There was an increase in the release rate afterward: this may be related to structural changes related to the sealing layer erosion by DMSO. Figure 3G and H present Cryo-SEM pictures obtained after 14 and 50 days of in vitro operation, respectively, for a capsule filled with 70% DMSO. These images illustrate the structural changes that occur over time in the sealing layer.

### 2.6. In Vitro Drug Release Study without External Triggering

To study the leakage of the different drug solutions packaged in the capsules (Solutions 1 to 8 in Table 1), the devices were immersed in PBS and the evolution of the drug concentrations released in the PBS with time was measured by UV–vis spectrometry. **Figure 4**A,C show the temporal evolution of the cumulative drug release of the four studied drugs (5-FU, DTX, DOX, CUR) dissolved in 70% DMSO (Solutions 1 and 3) and 30% DMSO (Solutions 2 and 4) respectively. The encapsulated drugs can be possibly released from the capsule through three different paths: 1. Permeation through the lipid sealing layer, 2. Permeation through the PEGDA-based reservoir, 3. Release through a gap between the sealing layer and reservoir. However, we have shown previously that the sealing layer and the reservoir are tightly attached without gaps (Figure 2B), and there is no apparent defect or pore in the sealing layer at the initial state (Figure 2E,F). 5-FU and DTX release through a reservoir sealed with epoxy was less than 2% for 50 days (Figure 4D), which is less than 10% of the cumulative released amount from the PEGDA reservoir sealed with the lipid layer during the same period (Figure 4A). This indicates that the permeation of drugs through the lipid sealing layer should be seen as the main cause of drug leakage from the capsules.

The release profile of 5-FU in both 70% (Solution 1) and 30% (Solution 2) DMSO through the sealing layer follows a similar trend to that of DMSO seen previously (Figure 3F). The initial release of 5-FU can be associated with the drug intake into the sealing layer during fabrication (Figure 3D). After the initial release, there was a period of slow and constant release that lasted 14 days for 70% DMSO and 35 days for 30% DMSO. Finally, the drug release rate increased after that period. This behavior

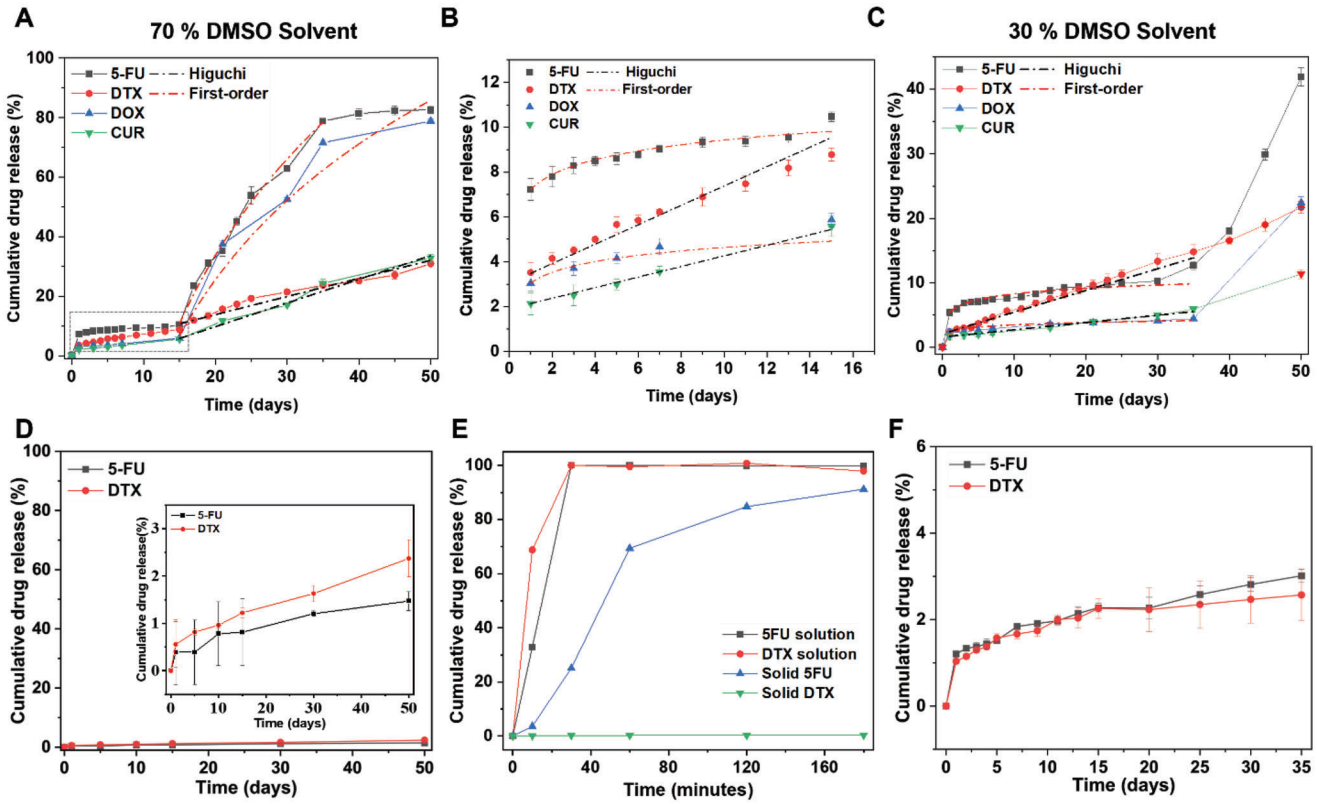


**Figure 4.** In vitro drug release study from the capsule. A) Drug release profile of 70% DMSO solvent-drug solutions (Solution 1,3 in Table 1) packaged capsule fitted with Higuchi model (black dash-dot line) and first-order model (red dash-dot line) B) Theoretically calculated drug release trend based on Higuchi model and first-order model fitted with experimentally obtained values from Figure 4A (black dot box). C) Drug release profile of 30% DMSO solvent-drugs solutions (Solution 2,4 in Table 1) packaged capsule fitted with theoretically calculated drug release trend based on Higuchi model and first-order model. ($n = 3$) D) Drug release through the PEGDA reservoir: Drug release profile of 5-FU and DTX from the 70% DMSO solvent-drugs solution packaged PEGDA reservoir sealed with epoxy. ($n = 3$) E) Drug release profile of the capsule containing solution and solid form of 5-FU and DTX without sealing layer. ($n = 3$) F) Drug release profile of capsule which packaged solid form of 5-FU and DTX. ($n = 3$).

correlates clearly with the one seen in Figure 3F for the permeation of DMSO alone, which is a strong indication that the release of 5-FU and DMSO are linked. In the case of 70% DMSO, the 5-FU release slowed down after 35 days and released 82% of encapsulated 5-FU. Degradation of the drugs during in vitro operation for 50 days and drug molecules binding to the sealing layer and micro-reservoir surface may contribute to the fact that the final released amount does not reach 100%. Figure S7 (Supporting Information) shows optical images of the capsules with 70% and 30% DMSO after 50 days of in vitro drug release. The drug release of DOX from the capsule (Figure S8, Supporting Information) (which has a similar affinity with water and DMSO as 5-FU) follows the same profile as 5-FU, both for solution in 70% DMSO (Solution 3) and 30% DMSO (Solution 4) with differences in drug release rates. This is coherent with their different diffusion and partition coefficients (**Table 2**, Supporting text 2).

The drug release profiles of DTX and CUR are different from the ones of DOX and 5-FU. In both 70% DMSO (Solutions 1 and 3) and 30% DMSO (Solutions 2 and 4), there is an initial release during the first day of ≈3% of the encapsulated drug due to the initial intake of drugs into the sealing layer during the fabrication (Figure 3D), this amount is smaller than in the case of 5-FU and DOX since DTX and CUR have a lower diffusion coefficient in the lipid layer than 5-FU and DTX (Table 2). In the case of 70% DMSO, both drugs released 30% of their encapsulated drugs after 50 days without significant changes in drug release rates, whereas for 30% DMSO, DTX released 20% and CUR released 10% of their encapsulated drugs after 50 days without significant changes in the drug release rate. Both DTX and CUR are highly lipophilic drugs and exhibit poor water solubility and limited solubility in DMSO. Unlike hydrophilic drugs, the release of DMSO did not affect the DTX and CUR release kinetics. The difference in their release behavior compared to 5-FU and DOX likely relates to their differences in solubility and hydrophilicity/lipophilicity.

To elucidate the drug release mechanism from the capsule, a semi-empirical analysis was carried out by applying different drug release models to the experiments presented in Figure 4A,C (Table S1, Supporting Text 3).[16] As we observed a change of behavior in the drug release rates after 14 days for 70% DMSO and after 35 days for 30% DMSO, the semi-empirical analysis was also divided into two parts accordingly. The model trend line with the highest $R^2$ value is considered to adequately account for the experiment results.

The first-order model, which follows Fick's diffusion law, adequately accounted for the release profile of 5-FU and DOX in all cases. The calculated drug release trends obtained from the

**Table 2.** Experimentally measured permeability, partition, and diffusion coefficient of 5-FU, DTX, DOX, and CUR dissolved in 70%, 30% DMSO concentration aqueous solvent through lipid and PEGDA membrane. (Methods explained in Supporting Text 2).

| | Permeability coefficient [$mm^2/day$] | Partition coefficient | Diffusion coefficient [$mm^2/day$] |
|---|---|---|---|
| 5-FU to lipid, 70% | $2.63 \times 10^{-6}$ | $1.85 \times 10^{-4}$ | $1.42 \times 10^{-2}$ |
| DTX to lipid, 70% | $4.27 \times 10^{-6}$ | 8.496 | $5.00 \times 10^{-7}$ |
| 5-FU to PEGDA, 70% | $4.29 \times 10^{-7}$ | $8.00 \times 10^{-4}$ | $5.36 \times 10^{-4}$ |
| DTX to PEGDA, 70% | $9.36 \times 10^{-6}$ | 0.194 | $4.83 \times 10^{-6}$ |
| DOX to lipid, 70% | $1.25 \times 10^{-6}$ | $1.28 \times 10^{-4}$ | $9.76 \times 10^{-3}$ |
| CUR to lipid, 70% | $3.85 \times 10^{-6}$ | 5.344 | $7.20 \times 10^{-7}$ |
| 5-FU to lipid, 30% | $2.20 \times 10^{-6}$ | $1.73 \times 10^{-4}$ | $1.27 \times 10^{-2}$ |
| DTX to lipid, 30% | $3.89 \times 10^{-6}$ | 8.537 | $4.58. \times 10^{-7}$ |
| DOX to lipid, 30% | $9.65 \times 10^{-7}$ | $9.90 \times 10^{-5}$ | $9.74 \times 10^{-3}$ |
| CUR to lipid, 30% | $2.18 \times 10^{-6}$ | 3.03 | $7.20 \times 10^{-7}$ |

first-order model equation (Equation S5, Supporting Text 4) are shown in Figure 4B,C (red dotted line) alongside experimental data, with an $R^2$ value higher than 0.95 indicating a good fit. The first-order release model depends on the changes in drug concentration inside the capsule.

The Higuchi model adequately accounted for the release profile of DTX and CUR in all studied cases. The Higuchi diffusion model is the best fit for the experimental data corresponding to conditions where a slow diffusion occurred through the sealing layer with a fast partition of drugs into the sealing layer. The calculated drug release trend obtained by the Higuchi model equation (Equation S6, Supporting Text 4) is shown with experimental data points in Figure 4B,C (black dotted line). The fact that drug release was independent of drug concentration changes in the reservoirs under conditions where the Higuchi model fit well with the experiments indicates that the sealing layer membrane that closes the reservoirs was replenished with drug molecules faster than they diffuse in the outer medium. This is consistent with the high partition coefficient and low diffusion coefficient measured for DTX and CUR.

Drug release profiles of capsules packaging one single drug only (Solutions 5 to 8) (Figure S9, Supporting Information) have similar release profiles as capsules packaging multiple drugs with different pharmacokinetics (Solutions 1 and 2). This demonstrates that encapsulating multiple drugs with different release pharmacokinetics does not affect the intrinsic drug release kinetics at least for the 4 drugs used in this study. This feature can be used to better adapt the therapy to the patient by simultaneous delivery of multiple combinations of drugs using a single capsule. Storing the capsule at −20 °C for 30 days did not change the release kinetics of the drugs from the capsule (Figure S10, Supporting Information), thereby directly supporting the negligible effect of capsule storage, which facilitates the capsule's distribution and long-term supply to the patient.

Figure 4E compares the release profiles of 5-FU and DTX from the capsule when these drugs are encapsulated either as solid powders or as drug solutions in 70% DMSO. In this experiment, the drugs were simply placed in the capsules without a sealing layer, and the capsules were then immersed in PBS. Both capsules containing drugs in solution released almost 100% of their cargo within 30 min. Capsules containing 5-FU in solid powder form released 85% of the drug within 3 h, while capsules containing DTX released only ≈0.3% of the drug in the same period due to its low water solubility. This indicates that delivering poorly water-soluble drugs in solution form directly can significantly enhance the efficiency of drug delivery.

Figure 4F shows the release profiles of 5-FU and DTX packaged as a solid powder in capsules, this time with a lipid sealing layer. After an initial burst release of ≈1% of the drugs occurring during the first day, the capsules are placed in PBS. Both drugs are released similarly for the following 35 days of the experiment, with a total cumulative drug release of ≈3% during this period. It verifies that the water permeation into the capsule is negligible, which means the fabricated capsule acts as a sealing barrier to protect the packaged cargo from the water environment. It also reveals the role of solvent in the drug release mechanism that maintains the partition of the drug into the lipid layer by physical contact. Packaging drugs in solid form is a good way to protect them from their environment as it has been seen that water permeation through the lipid layer is minimal.

### 2.7. Magnetically Triggered Heating of the Capsule

**Figure 5**A shows the evolution of the temperature of the top surface of the capsule's sealing layer subjected to an AMF at a frequency of 111 kHz and intensity of 24 mT in air. Figure 5B shows the corresponding IR temperature images. The temperature of the sealing layer increased up to 40 °C in 5 min and remains constant at ≈40 °C for 30 min. The stabilization of the temperature at 40 °C is a sign of a phase transition of the sealing layer. After the phase transition, the temperature increased to 47 °C due to the Brownian relaxation mechanism related to the rotation of the magnetic nanoparticles in the melted lipid matrix. The duration required for melting the sealing layer can be controlled by the concentration of the magnetic nanoparticles in the lipid layer, as well as by the frequency and intensity of the magnetic field.[17]

The heating process of the sealing layer can cause changes in temperature in both the packaged drugs and surrounding tissues (when the capsule is implanted). Potentially resulting in drug degradation and tissue damage. To investigate this, temperature changes were measured in a larger version of the capsule (made

 

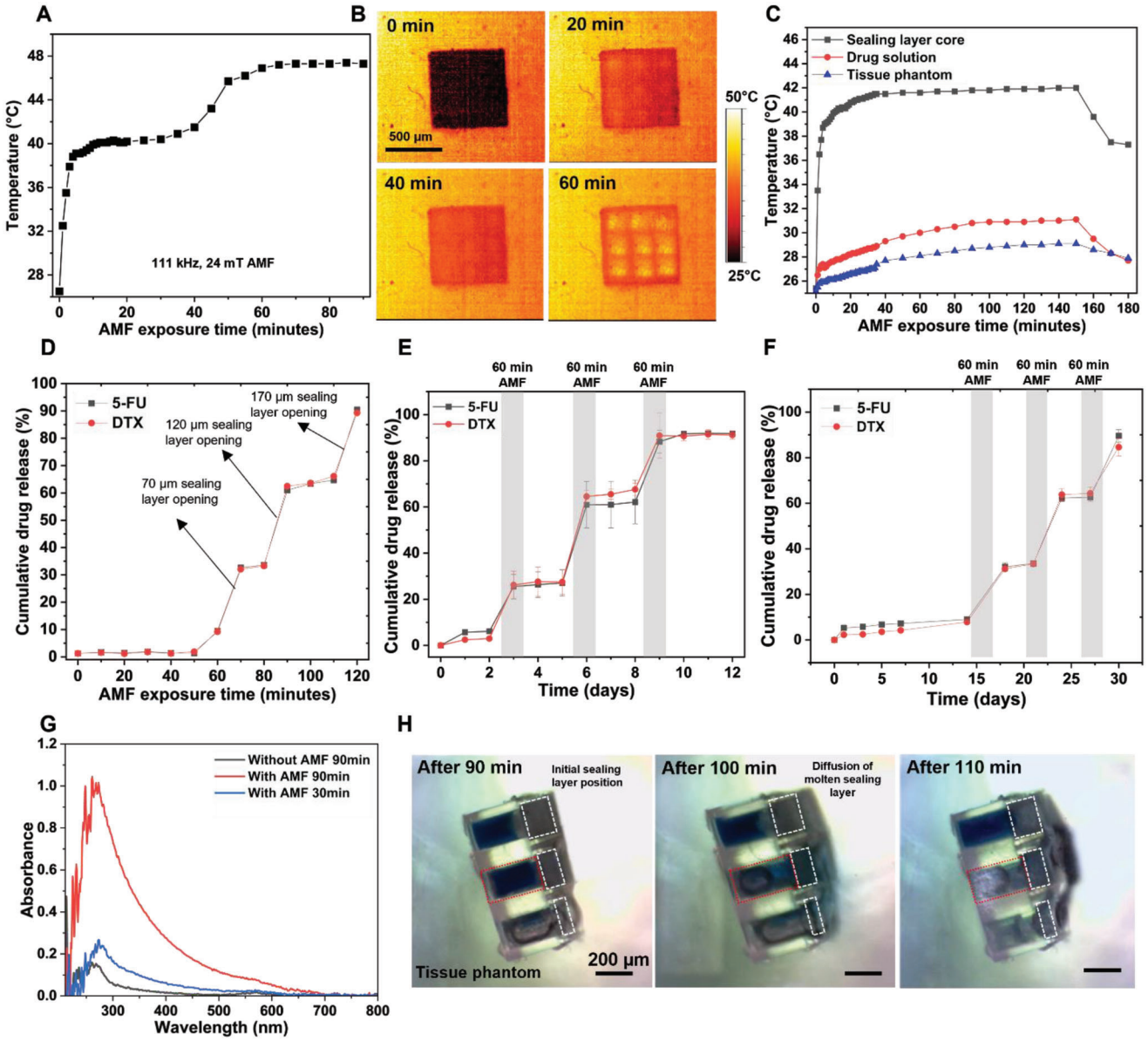


**Figure 5.** In vitro Magnetically triggered drug release study from the capsule. A) Temperature change of the sealing layer surface in air under AMF exposure over time, and B) corresponding IR images. C) Temperature changes of the macro capsule model placed in tissue phantom under AMF exposure: sealing layer's surface, drug solution, and tissue phantom contact with sealing layer. D) Drug release profile of 70% DMSO solvent-drugs solution packaged capsule under continuous AMF exposure in PBS, each pulsatile drug release corresponds with the opening of sealing layer with different thickness. E) Drug release profile of wirelessly active drug release control from 70% DMSO solvent-drugs solution packaging capsule for 12 days by exposing AMF at 3,6, and 9 days. ($n = 3$) F) Wirelessly active drug release control from 30% DMSO solvent-drugs solution packaged capsule for 30 days by exposing AMF at 17, 23, and 29 days. ($n = 3$) G) AMF triggered drug release of the capsule in cancer tissue-mimicking phantom: UV absorbance of tissue phantom with and without AMF exposure, H) and optical images of the capsule in tissue phantom under AMF exposure.

from one well from a 96-well strip plate with the same contact area to liquid volume ratio as the microcapsule) using an optical temperature sensor (Figure 5C). During 150 min of exposure to the AMF, the temperature in the sealing layer increased from 26 to 42 °C, while the temperature of the packaged liquid and the tissue phantom changed to a lesser extent, from 26 to 32 °C and from 26 to 28 °C, respectively. After 150 min, the sealing layer melted, and the molten sealing layer diffused into the surrounding tissue. The diffusion of the molten sealing layer is followed by a general drop in temperature in all materials probed, thereby regulating the maximum temperature to 42 °C. This feature can be utilized as a self-regulatory function of the device to avoid overheating of the surrounding tissue. It should be noted that this experiment provides only a preliminary indication of the temperature evolution in and around the microcapsule. Because it was conducted using a larger device at the mm scale (Figure S11, Supporting Information), which may result in slower temperature changes than in the microenvironment. In addition, our

experiments were conducted at room temperature (24 °C), not at physiological temperature. Nonetheless, these results indicate that the temperature changes remain of limited magnitude and are unlikely to induce significant drug degradation or tissue damage, as normal tissue does not sustain significant damage when exposed to 44 °C for 1 h.[18]

### 2.8. Magnetically Triggered Sealing Layer Opening and Drug Release Study

Figure 5D shows the temporal evolution of the release of 5-FU and DTX from Solution 1 packaged in the microcapsule placed in PBS during continuous AMF exposure. Three release events of both drugs were observed, which occurred after 60, 80, and 100 min. The release of the drugs in PBS is fast and takes place within ≈10 min. The sequential release of both drugs corresponds to the dissolution of the molten sealing layers of different thicknesses, with the thinner sealing layers (70 µm in thickness) opening first after 60 min, the medium one (120 µm in thickness) opening after 80 min, and the thickest (170 µm in thickness) opening last, after 100 min.

Figure 5E shows the temporal evolution of the release of 5-FU and DTX in 70% DMSO from capsules placed in PBS for which the AMF is exposed for 60 min only at chosen time points on days 3, 6, and 9, respectively. The concentration of the drug was measured 60 min after the AMF exposure. Each triggering step allows the opening of a set of reservoirs with a different sealing layer thickness (Figure S12, Supporting Information), which results in a sequential release of the drugs contained in the capsule on demand. Only a very limited amount of drug leaks from the capsules between the triggering events (less than 1%). Confronting the time needed to open the capsule with the one shown in Figure 5D, it turns out that at each exposure to AMF, some of the unopened sealing layer is lost (Figure S12, Supporting Information). However, this thinning of the sealing layer does not result in unwanted release. Figure 5F is like Figure 5E, for drugs in 30% DMSO. Here the release is triggered after long durations on days 17, 24, and 29. The actively controlled release of multiple drugs over their pharmacokinetics in a programmable manner for a prolonged time from the single capsule can be achieved by controlling AMF exposure.

To investigate the opening of the sealing layer and the subsequent drug release in conditions like these of a capsule implanted in tissues, tissue phantoms were prepared, made of 1.5% agarose and 0.5% sodium alginate in water. The obtained gel is known to have mechanical properties like cancerous tissues.[19] Capsules filled with Solution 1 were placed in such tissue phantoms directly solidified inside spectroscopy cuvettes. Figure 5G shows the evolution of the absorbance in the prepared cuvettes before and after their exposure to the AMF used for opening the sealing layer, for 30 and 90 min. The increase of the peak of UV–vis absorbance at ≈260 nm can be observed over time and is related to the sequential opening of the reservoirs and the release of the drug it contains in the capsule. Figure 5H shows the diffusion of molten sealing layers into the tissue phantom, and the release of the drug solution encapsulate by 120 µm sealing layer under continuous AMF exposure, while the drug solution encapsulated by 170 µm sealing layer is not released despite the diffusion of the molten sealing layer. This reveals that the sequential opening of the sealing layers according to their thickness is caused by the difference in the time it takes for the molten sealing layer to completely diffuse into the tissue phantom.

### 2.9. In vitro Demonstration of a Capsule and its Drug Release Effect on Cells

The effect of the capsule opening and the release of the drug solutions they contain was evaluated on different cell lines in vitro. A375 (human epidermal cancer cell line) and HACAT (human epidermal cell line) were cultured for 3 days before capsules filled with Solution 1 were inserted in the cell cultures such that their sealing layer was placed in contact with the cells (Figure S13, Supporting Information). After the capsule was inserted, the cells were cultured for 6 additional days and exposed to an AMF for 60 min on days 1, 3, and 5 as illustrated by the gray zones in **Figure 6**A,C, leading to the sequential opening of the different reservoirs. Presto blue cell viability assays were performed on the cell cultures 24 h after the reservoir opening is triggered, as shown in Figure 6A,C. It clearly shows the decrease in cell viability with each subsequent reservoir opening in the case of both cell lines. Control experiments show only a very limited decrease of cell viability when the capsule does not contain drug and only the capsule opening mechanism (AMF exposure) and solvent affects the cell viability (noted +AMF/-Drug) or when a capsule that contains drugs is never opened by AMF (noted -AMF/+Drug) after day 1. The reason for the significant drop in cell viability on day 1 in the -AMF/+Drug group is due to the initial burst release of the drug.

Figure 6B,D show fluorescence images of cells in culture submitted to the same protocol described previously in the case of Figure 6A,C, but for different cell viability assays. In these figures, the top rows show cells dyed with fluorescein-5-isothiocyanate (FITC) and cyanine3 (CY3) where green fluorescence indicates live cells and red indicates dead cells, while the bottom rows show cells dyed with 4′,6-diamidino-2-phenylindole (DAPI) that stains the nucleus of live cells in blue. There was a decrease in cell viability with each subsequent exposure of the cells to drugs on days 2, 4, and 6, as the staining of the cells is performed 24 h after one set of reservoirs is opened by subjecting the capsule to an AMF (labeled +AMF/+Drug). The same control experiments as in Figure 6A,C are also performed and the corresponding pictures taken on day 6 are shown in Figure 6B,D (labeled +AMF/-Drug and -AMF/+Drug similarly as described in the previous paragraph). Fluorescence images of cells from control experiments on days 2 and 4 are shown in Figure S14 (Supporting Information). These control experiments show good viability of the cells that is coherent with Presto blue cell viability assay results (Figure 6A,C).

For the two types of cells cultured, Figure 6E compares the cell viability on day 6 using the Presto blue viability assay. When no drug is present in the capsule, the cell growth does not show a significant difference after 6 days, with or without a capsule in contact with the cells and with or without opening of the capsule by the AMF exposure. It indicates that the capsule components and the solvent are nontoxic to cells and the effect of AMF and AMF-induced heat is negligible on cells. When drugs are present

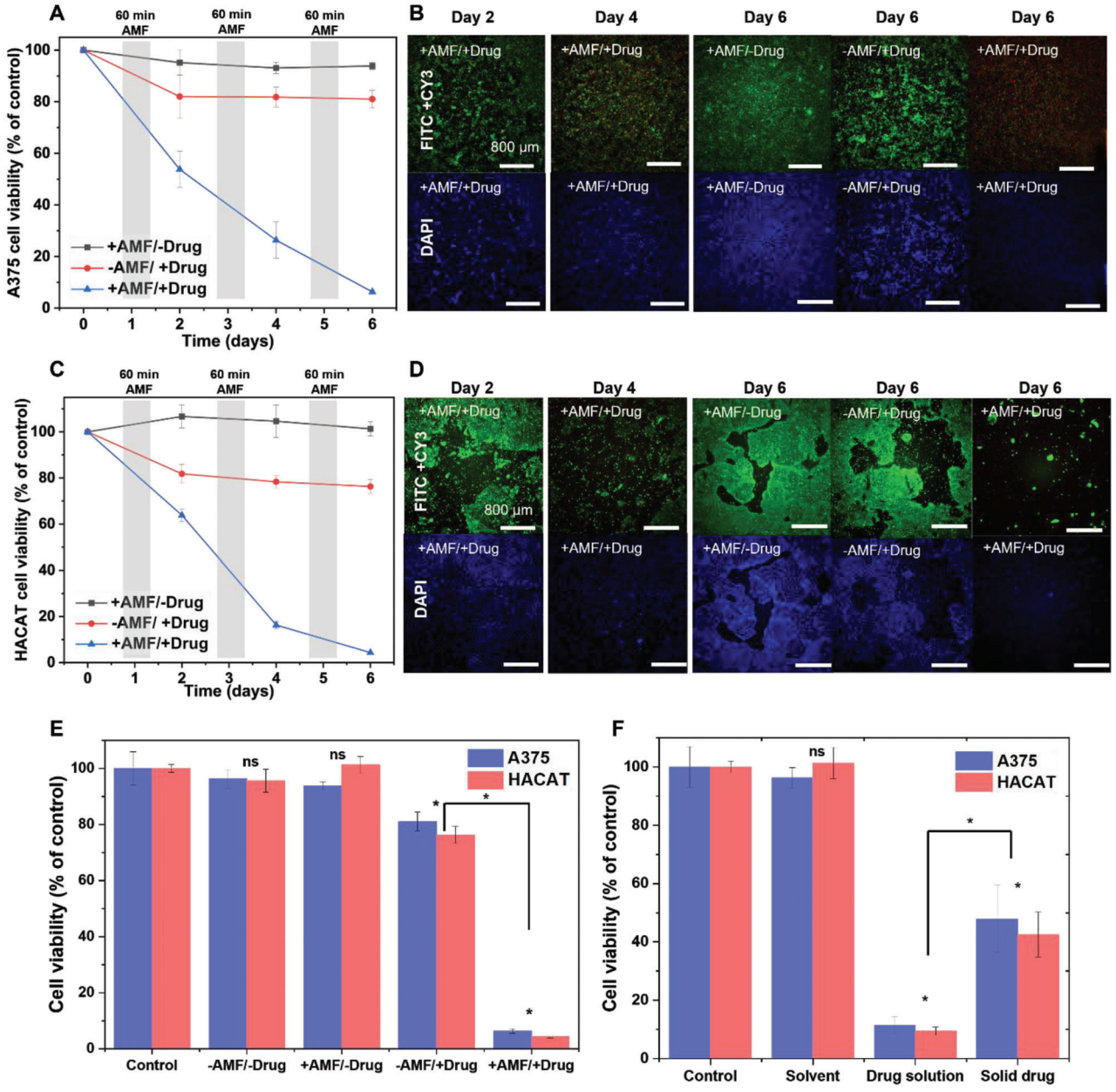


**Figure 6.** In vitro demonstration of the capsule's-controlled drug release feasibility in oncology application. A) Presto blue fluorescence-based cell viability of A375 cells and C) HACAT cells incubated with capsule encapsulating drug solution with (+AMF/+Drug) and without (-AMF/+Drug) AMF exposure, and capsule encapsulating solution without drugs with AMF exposure (+AMF/-Drug) for 6 days. ($n = 5$) And corresponding fluorescence images of B) A375 and D) HACAT cells stained with FITC/CY3, and DAPI. E) Statistical analysis of presto blue fluorescence-based cell viability of A375 and HACAT cells under different conditions +AMF/+Drug, +AMF/-Drug, -AMF/+Drug, and -AMF/-Drug on day 6. (*$p < 0.05$; ns, $p > 0.05$; $n = 5$) F) Statistical analysis of the presto blue fluorescence-based cell viability of A375 and HACAT cells incubated with a capsule containing drug solvent, drug solution, and the solid drug without sealing layer after 1 day. (*$p < 0.05$; ns, $p > 0.05$; $n = 5$)

in the capsule, cell viability is affected, when the reservoirs remain closed as some of the drugs gradually release over time, and even more when they are opened and the drug they contain is released. Corresponding fluorescence images supporting our experimental results are shown in Figure S15 (Supporting Information).

Figure 6F compares the cell viability 24 h after the cells are subjected to different conditions: Cells without any perturbation constitute the control, cells in contact with an open capsule containing only the 70%DMSO (Solvent), cells in contact with an open capsule containing Solution 1 (Drug solution), and cells in contact with an open capsule containing solid drugs in the same amount as Solution 1 (Solid drug). Again, only the presence of drugs has a significant impact on cell viability, with a much larger impact on cell viability after 24 h observed for drugs in solution compared to drugs in solid form, which is coherent with the

release profile presented in Figure 4E. Corresponding fluorescence images of the experiments are shown in Figure S16 (Supporting Information).

## 3. Discussion

We have developed a new technological approach to package nL volumes of liquid accurately inside a microcapsule that contains multiple reservoirs for drug delivery as its target application. The developed fabrication process results from the combined use of advanced additive micro-manufacturing technologies: TPP for the reservoir fabrication and dual IJP for reservoir filling and sealing. Our work presents a first, but significant step toward new liquid handling strategies, and our results may trigger further research along this line toward engineering of components made by additive manufacturing for in vivo applications. Here we used a resin based on PEGDA that is bioresorbable and biocompatible but that is not yet approved for implantation by FDA and other regulatory bodies. We are also aware that further development of the resins used for TPP is still needed before this technology can be considered for implants. The high versatility of additive manufacturing also means that this technology can be applied to other biomedical applications beyond drug delivery, such as lab-on-chip and analytical systems.

The use of dual IJP for filling and sealing the reservoirs is of great interest as it solves many of the problems encountered in previous attempts to develop nL liquid packaging in microsystems. IJP allows for precise dispensing of pL volumes of liquid inside the reservoirs, minimizing cargo waste and enabling precise dosage of dispensed volumes. Additionally, IJP minimizes liquid evaporation during the fabrication process as the sealing layer can also be dispensed by IJP after a delay of only a few seconds. This is advantageous as the liquid dispensing and packaging processes do not involve high temperature, UV-irradiation, or organic solvents, which can affect the cargo. IJP also allows for high flexibility in materials, enabling the packaging of liquid cargos other than drug solutions, such as colloidal emulsions or nanoparticle suspensions. In the implementation presented in this work, a sealing layer made of lipids mixed with magnetic nanoparticles was dispensed on top of a drug solution in a molten form. The spreading of the sealing layer above the aqueous solution by the Marangoni effect was based on a simple and well-controlled process. The solvent used to dissolve the drugs in this study was a mixture of DMSO and water. While water is immiscible and impermeable with the lipids used, the same is not true for DMSO or drugs. As a result, some amount of DMSO and drugs can migrate into the lipid layer during solidification, leading to an initial burst-release of these components followed by continuous slow permeation of DMSO and drugs through the capsule in the operating environment. This effect can be viewed as a drawback or an asset, depending on the context. On one hand, it limits the precise temporal control over the release of the packaged components. On the other hand, it can be leveraged to provide a passive release of hydrophilic drugs as a secondary drug release mechanism, in addition to the burst release obtained by opening the sealing layer.

The produced capsule contains multiple independent reservoirs with varying sealing layer thicknesses, which allow them to be opened sequentially on demand using AMF. The drug release mechanism, which is based on the sequential removal of the molten sealing layer by AMF, has been demonstrated in a liquid environment (PBS) and tissue phantoms with mechanical properties like those of cancer tissue. However, before using such a device in a medical context, further in vivo studies need to be conducted to validate its function once implanted. The release mechanism can be further adjusted to accommodate additional delivery steps by varying not only the thickness of the sealing layer deposited to close each reservoir but also the concentration of MNP mixed with the lipids.

The capability of wirelessly controlling multiple releases of cargo from the capsule provides unprecedented flexibility in drug release from a single capsule. It allows for precise control over the opening of each reservoir, enabling customization of the drug release profiles, and thereby facilitating personalized drug delivery. It also allows for choosing the dosage of each drug release event after the capsule has been implanted by defining the number of reservoirs opened simultaneously. Direct drug solution release can enhance the therapeutic effect of poorly water-soluble drugs and increase the variability and efficacy of the therapy by delivering multiple drugs simultaneously. In addition, the different reservoirs can be filled with different drugs for improved therapeutic flexibility. However, the capsule has a limitation due to its bioresorbable properties: once implanted, all the drugs contained in the capsule will eventually be released into the patient's tissues. It is not possible to permanently close some of the reservoirs or stop administering the drugs they contain. Additionally, enzymatic degradation of the lipid layer may compromise its ability to seal in vivo, which could increase the rate of drug release from the capsule and reduce its lifespan.

The in vitro cell experiments performed in our study demonstrate the potential of microcapsules for drug delivery as chemo implants with localized on-demand drug release control, increasing the effectiveness of drug delivery through direct solution administration. The drugs used in the present study were typical cancer treatment drugs, however, such capsules have the potential for drug delivery applications other than cancer treatment, by packaging other therapeutic compounds such as anti-inflammatory drugs or drugs used for psychotherapies. The amount of drug delivered is determined by the volume of the reservoir, concentration, and stability of the drug solution. In cases where higher doses are required, increasing the reservoir volume or number can increase drug loading but may compromise the minimal invasiveness of the capsule. Applying our nL liquid packaging technology to drug delivery applications paves the way for advanced micro drug delivery implants with the following advantages: It is small enough to be injected into the body with minimal invasion through a syringe, and no further surgery is required after implantation since it is made of fully bioresorbable materials. It can deliver multiple drugs with programmable control for prolonged periods according to their pharmacokinetics.

## 4. Experimental Section

*Fabrication of Bioresorbable Capsules*: The PEGDA-based photoresist was prepared by mixing PEGDA ($M_n$ = 250), pentaerythritol tetraacrylate (PETA), and Irgacure-369 (Sigma–Aldrich, St. Louis, MO, USA) with an

85:14.5:0.5 wt.% ratio. The photoresist was drop casted on a silicon substrate and positioned into the TPP tool (Photonic Professional GT; Nanoscribe GmbH, Eggenstein-Leopoldshafen, Germany). TPP was carried out with a wavelength of 390-nm, 17 mW power laser using a 10 times magnification lens. The photoresist was exposed with the 3D design defined in an STL file. The printing time of the single reservoir is six minutes. The non-exposed photoresist was developed by propylene glycol methyl ether acetate (Sigma–Aldrich, St. Louis, MO, USA) for 15 min and rinsed with isopropanol for 3 min. The obtained capsule was treated with an $O_2$ plasma of 200 W for 30 s.

*Liquid Packaging Inside the Capsule*: Drug solutions were prepared by dissolving different drugs 5-FU, DTX, DOX, and CUR (Sigma–Aldrich, St. Louis, MO, USA) in DMSO (Merck & Co., Kenilworth, NJ, USA) mixed with water at different ratios. All water used in this paper was distilled water. All prepared drug solutions were mixed for 20 min using a vortex mixer and 5 min with an ultrasound sonicator. The lipid layer was prepared by mixing 0.5 wt.% lecithin (Sigma Aldrich, St. Louis, MO, USA) with bio-grade lipid (Suppocire CM; Gattefosse SAS, Lyon, France) at 50 °C for 20 min. The $Fe_3O_4$ MNPs (100 nm lipid coated; Chemicell GmbH, Berlin, Germany) were added with a concentration of 8 wt/vol% in the melted lipid mixture and mixed for 20 min using a vortex mixer and 15 min by ultrasound sonication. The prepared drug solutions and the lipid-MNP mixture were dual inkjet printed by an automatic inkjet printer (JetlabII, MicroFab Technologies, Inc., Plano, TX, USA). The temperature of the lipid-MNP mixture reservoir, connection tube, and print head was maintained at 65, 70, and 50 °C, respectively, during printing.

*Cryo-SEM of Capsules*: For cryo-SEM imaging, the capsules were placed in a 3 mm diameter support (M. Wohlwend GmbH, Sennwald, Switzerland) together with a cryo-protectant solution (dextran 40 in M-solution (20% w/v), Sigma–Aldrich, St. Louis, MO, USA). The loaded support was vitrified within milliseconds by using a high-pressure freezing system (Leica EM ICE). The support was fixed in the cryo-SEM holder in a liquid nitrogen workstation (Leica EM VCM) and trimmed while operating a cryo ultramicrotome (Leica EM UC7) at −110 °C. This step consists of cryo planning the sample, to do so the top 80 um of the sample was removed using a trim knife (Diatome, Hatfield, PA, USA). The cryo-SEM holder was transported to a cryo e-beam coater (Leica EM ACE 600) in a vacuum cryo transfer system (Leica VCT500) keeping it in a vacuum and at −170 °C. A freeze etching process (also known as ice sublimation) was necessary to remove the ice crystal layer that formed on the surface. The sample was warmed up to −93 °C for 20 min at 3 °C $min^{-1}$ and kept at −93 °C for 1 min, to then bring it back steadily (3 °C $min^{-1}$) to −150 °C. After this step, the sample was coated with 3 nm of Pt (e-beam coating) for better imaging contrast with the SEM (Zeiss GeminiSEM 500). The cryo-SEM stage was maintained at −140 °C and the images were taken using the in-lens detector, at an energy of 1.7 keV and with an aperture of 10 mm. The working distance was set at 4.5 mm for optimized resolution.

*XPS*: PEGDA layers were manually detached from the lipid layer before analysis by XPS (Kratos Analytical Ltd, Manchester, UK) with 225 W excitation power (on the anode, not X-rays, which was not given as it fluctuates greatly during the lifetime of the anode), X-ray area of 400 × 700 $\mu m^2$, and exposure time of 1 h for each sample.

*Water Contact Angle Measurement*: The water contact angle was measured 10 s after water drop casting using Krüss DSA-30E (KRUSS GmbH, Germany).

*TGA Measurement of Capsules*: TGA of the capsules packaging Solution 2 was measured under $N_2$ environment. After keeping the sample for 1 min at 30 °C, the temperature was increased from 30 to 180 °C at 5 °C $min^{-1}$. Then the temperature was maintained for 20 min at 180 °C followed by a ramp from 180 to 700 °C at 5 °C $min^{-1}$, and the temperature was held for 10 min at 700 °C.

*LC-MS Analysis*: For LC, drug solutions were diluted at a 1:20 ratio using 0.1% formic acid in water. The separation was performed using a column of 2.1 mm diameter and 100 mm height (HSST3). For each measurement, 2 µL of sample was injected into the column, and each sample was injected in duplicate. Two mobile phases: A: 0.1% formic acid in water, and B: 0.1% formic acid in acetonitrile were mixed in different ratios according to the gradient condition. The gradient condition of the LC was started at 1% B for 1.7 min, then ramped to 80% B in 0.3 min, held 80% B for 1 min, ramped to 95% B in 0.5 min, and held 95% B for 0.5 min. Returned to initial 1% B conditions in 0.5 min and then equilibrated for 2.5 min. The mobile phases were injected into the column with a 0.4 mL $min^{-1}$ flow rate.

MS was performed using an Exploris ™240 Orbitrap interfaced with the HESI ionization source in negative mode (0 to 2 min) and then in positive mode (2 to 7 min). MS spectra were acquired in the 100–1200 m/z mass range at a resolution set to 120k, with the mild trapping option and 2 µscans, with ion transfer tube temperature at 325 °C. The peak area of the XIC chromatograms (MEW 50 ppm) for the 2 main ion species (m/z: 129.0107 for 5-FU and 808.3539 for DTX) was integrated for the quantification of the 5-FU and DTX in the sample.

*In Vitro DMSO Permeation Measurement*: To evaluate the permeation of DMSO, capsules filled with 30% and 70% DMSO were incubated in 200 µL of PBS at 37 °C for 50 days. At each time point, the supernatant was withdrawn, and its UV absorbance was measured by a UV–vis spectrophotometer (NanoDrop™ 2000c Spectrophotometers, Thermo Fisher Scientific, Waltham, MA, USA). The DMSO concentration was calculated by integrating the area under the measured curve from 200 to 250 nm wavelength.

*Measurement of the Erosion and Solvent Intake in the Lipid Membrane*: A lipid membrane 200–300 µm in average thickness was prepared by drop casting 10 µL of lipid heated at 50 °C on the surface of 70% DMSO, and PBS (PBS, pH 7.4, Thermo Fisher Scientific, Waltham, MA, USA) and solidified at 25 °C. The lipid membranes floating on the liquid surface were incubated at 37 °C, 30 rpm in an orbital shaker. At each measurement point, the membranes were withdrawn from the liquid, then the remaining liquid on their surface was carefully removed, and their weight was measured (wet mass). Then the membranes were placed in a vacuum chamber for 3 days to dry them, and their mass was measured again (dry mass). Erosion was calculated by dividing the dry mass minus the initial mass by the initial mass. And solvent uptake was calculated by dividing the wet mass minus the dry mass by the dry mass.

*Degradation and Water Content Measurement of Polymerized PEGDA-Based Material*: Ten cubes with a dimension of 260 µm in the X, Y, and Z axis, made by TPP using the same PEGDA-based photoresist used for the fabrication of the micro reservoir, were placed in a centrifuge tube with 1 mL of PBS, and 1 mL of 70% DMSO in water for one-time point measurements. The tubes were incubated at 37 °C, with a 30 rpm orbital shaker. For each measurement, the cubes were centrifuged and washed with DI water 3 times. The cubes were withdrawn from the water, then the remaining water on their surface was removed. TGA measurement was performed in an $N_2$ environment with a temperature ramp from 30 to 700 °C with temperature held at 180 and 430 °C for 20 min. The remaining cube mass was obtained by subtracting the mass measured after maintaining the temperature at 180 °C and the water intake in the cube was calculated by subtracting the mass measured after maintaining the temperature at 180 °C from the initial mass.

*In Vitro Drug Release Measurement*: For all in vitro drug release experiments, five capsules filled with drug solution of different drugs (5-FU, DTX, DOX, CUR) with different DMSO concentrations (30%, 70%) were placed in a 2 mL micro-centrifuge tube containing 200 µL of PBS incubated at 37 °C, 30 rpm orbital shaker. The supernatant was withdrawn, and its UV absorbance was measured at each measurement point with PBS as a blank using a UV–vis spectrophotometer (NanoDrop 2000C) that allows identifying the main absorption peaks of the four drugs used in this study (5-FU:265 nm, DTX:227 nm, DOX:485 nm, CUR:425 nm). After each measurement, the tubes were refilled with fresh PBS. At each measurement point, the concentration of each drug present in the supernatant was obtained using a previously established calibration curve. Comparing these measurements to the initial concentration of each of the drugs packaged in the capsule allows us to establish the cumulative drug release profile with time. Drug-loaded capsules sealed with epoxy were prepared to investigate the drug release through the PEGDA-based reservoir. Capsules loaded with drugs in solid form rather than dissolved in solvents were prepared. In that case, the capsules were first loaded with drugs in solution and then placed in a vacuum chamber for 3 days to evaporate the solvent.

Capsules that packaged drugs in solid form were prepared by placing the drug solution packaged capsule that was prepared as same as the drug solution packaged capsule used for in vitro drug release measurement in a vacuum chamber for 3 days.

*Magnetically-Triggered Drug Release Study*: Five capsules filled with drug solutions were placed in a 2 mL centrifuge tube filled with 200 µL PBS. The tubes were thermally insulated by a Styrofoam case and exposed to AMF with a frequency of 111 kHz and 24 mT intensity using a MagneTherm system (Nanotherics Ltd, Warrington, UK) at a designated time point. Before and after exposure to AMF, the samples were incubated at 37 °C, 30 rpm in an orbital shaker condition. The drug concentration was measured right after the AMF exposure using a UV–vis spectrophotometer as same as the in vitro drug release measurement.

*In Vitro Drug Release Study in Tissue Phantoms*: The cancer tissue-mimicking phantom was prepared by dissolving 1.5% agarose, and 0.5% sodium alginate (Sigma–Aldrich, St. Louis, MO, USA) in water and heating the mixture using a microwave at 700 W for 10 s, then cooled down to 40 °C. 750 µL tissue phantom solution was poured into UV cuvette (Semi micro cuvette, BrandTech Scientific, Inc., Essex, UK) and solidified. Five drug solution packaged capsules were placed on top of the obtained hydrogel layer and 750 µL tissue phantom solution was poured above the capsule and solidified. Drug release from the capsules and drug concentration measurements were performed similarly as previously presented, with a tissue phantom prepared without capsules as a reference for UV-absorbance measurement.

*Magnetically-Triggered Temperature Changes Study*: The temperature of the capsule's sealing layer surface when exposed to AMF was measured with an IR thermal camera (Microscope optics, Optris GmbH, Berlin, Germany), and the temperatures of the drug solution, agarose gel, and in the center of the sealing layer were measured using optical fiber temperature sensors (PRB-100 OSENSA's fiber optic, OSENSA Innovations Corp., Burnaby, Canada), which were placed inside the agarose gel, and sealing layer before their solidification.

*In Vitro Cell Viability Study*: A375 and HACAT cells were cultured in RPMI 1640 growth medium (Thermo Fisher Scientific, Waltham, MA, USA) mixed with 10% fetal bovine serum (Thermo Fisher Scientific), 100 g $mL^{-1}$ of penicillin (Thermo Fisher Scientific), and 10 g $mL^{-1}$ of streptomycin (Thermo Fisher Scientific). Both cell lines were seeded in a flat-bottomed 96-well strip plate (Corning Inc., NY, USA) with $1 \times 10^4$ cells $mL^{-1}$ concentration (100 µL). Cells were incubated at 37 °C, 5% CO2, and humidity exceeding 80% for 3 days to sufficiently proliferate before the addition of the capsule. Five capsules filled with drug solutions were sterilized by spraying 70% EtOH on the surface before use. The stripped wells were sealed with a breathable film and placed into a sterilized Styrofoam thermal insulation cage, before placing it in the AMF generator (MagneTherm). Cell proliferation was measured 24 h later. The cell medium was also changed 24 h after exposure to the AMF.

Cell viability assay was performed by dispensing 10 µL prestoblue reagent (Thermo Fisher Scientific, Altham, MA, USA) on the cells, which were subsequently incubated for 1 h at 37 °C. The fluorescence was measured with Tecan Sunrise (Tecan, Männedorf, Switzerland) with excitation and emission wavelength of 560–590 nm, respectively. Live/dead cell allays were performed by Fluorescence cell images were taken by staining cells with fluorescein-5-isothiocyanate (FITC) (green color for live cells) + cyanine3 (CY3) (red color for dead cells) and 4′,6-diamidino-2-phenylindole (DAPI) (blue color for live cell's nucleus) dyes for 30 min and their fluorescence was imaged using an IN-Cell Analyzer 2000 (GE Healthcare, Chicago, IL, USA).

*Statistical Analysis*: Data collected by at least three independent experiments were presented as the mean ± standard deviation. The significant difference between sample groups was determined by one-way ANOVA with Tukey's for post-hoc analysis. For all analyses, statistical significance was expressed as a *p*-value, *p*-value smaller than 0.05. (* $p < 0.05$) was considered statistically significant. All data were analyzed using Microsoft Excel (Microsoft, Redmond, WA, USA).

## Supporting Information

Supporting Information is available from the Wiley Online Library or from the author.

## Acknowledgements

The authors especially thank Marc Chambon, Nathalie Ballanfat, and Fabien Kuttler for their help in the cell viability test and fluorescence imaging. The authors also thank Laure Menin for LQ-MS analysis for drug degradation analysis and Mounir Mensi for XPS analysis. Part of this work has received funding from the European Research Council (ERC) under the European Union's Horizon 2020 research and innovation program (Grant No. ERC-2016-ADG, Project "MEMS 4.0" Grant No. 742685). The authors have no conflict of interests.

Open access funding provided by Ecole Polytechnique Federale de Lausanne.

## Conflict of Interest

The authors declare no conflict of interest.

## Data Availability Statement

The data that support the findings of this study are available from the corresponding author upon reasonable request.

## Keywords

additive manufacturing, bioresorbable materials, controlled release, drug delivery, liquid-in-MEMS

Received: March 1, 2023
Revised: April 3, 2023
Published online:

[1] a) D. Chen, M. Mauk, X. Qiu, C. Liu, J. Kim, S. Ramprasad, S. Ongagna, W. R. Abrams, D. Malamud, P. L. Corstjens, *Biomed. Microdevices* **2010**, *12*, 705; b) T. van Oordt, Y. Barb, J. Smetana, R. Zengerle, F. von Stetten, *Lab Chip* **2013**, *13*, 2888.
[2] J. Hoffmann, D. Mark, S. Lutz, R. Zengerle, F. von Stetten, *Lab Chip* **2010**, *10*, 1480.
[3] a) R. Farra, N. F. Sheppard Jr, L. McCabe, R. M. Neer, J. M. Anderson, J. T. Santini Jr, M. J. Cima, R. Langer, *Sci. Transl. Med.* **2012**, *4*, 122ra21; b) J. Fong, Z. Xiao, K. Takahata, *Lab Chip* **2015**, *15*, 1050; c) J. Koo, S. B. Kim, Y. S. Choi, Z. Xie, A. J. Bandodkar, J. Khalifeh, Y. Yan, H. Kim, M. K. Pezhouh, K. Doty, *Sci. Adv.* **2020**, *6*, eabb1093.
[4] a) J. T. Santini, M. J. Cima, R. Langer, *Nature* **1999**, *397*, 335; b) D. K. Armani, C. Liu, *J. Micromech. Microeng.* **2000**, *10*, 80.
[5] a) Y. Okayama, K. Nakahara, X. Arouette, T. Ninomiya, Y. Matsumoto, Y. Orimo, A. Hotta, M. Omiya, N. Miki, *J. Micromech. Microeng.* **2010**, *20*, 095018; b) A. Vastesson, M. Guo, T. Haraldsson, W. van der Wijngaart, *Sens. Actuators, B* **2018**, *267*, 111.
[6] M. W. Lam, S. A. Mabury, *Aquat Sci* **2005**, *67*, 177.
[7] a) S. Matsumoto, N. Ichikawa, in *2008 IEEE 21st International Conference on Micro Electro. Mechanical Systems*, IEEE, **2008**, 415; b) N. Miki, *Advances in Micro/Nano Electromechal Systems and Fabrication Technologies* **2013**, *2*, 41.
[8] S. Coppola, G. Nasti, V. Vespini, L. Mecozzi, R. Castaldo, G. Gentile, M. Ventre, P. A. Netti, P. Ferraro, *Sci Adv* **2019**, *5*, eaat5189.

[9] a) C. B. Fox, Y. Cao, C. L. Nemeth, H. D. Chirra, R. W. Chevalier, A. M. Xu, N. A. Melosh, T. A. Desai, *ACS Nano* **2016**, *10*, 5873; b) A.-V. Do, K. S. Worthington, B. A. Tucker, A. K. Salem, *Int. J. Pharm.* **2018**, *552*, 217.
[10] M. Browning, S. Cereceres, P. Luong, E. Cosgriff-Hernandez, *J. Biomed. Mater.* **2014**, *102*, 4244.
[11] a) L. Galanti, M. P. Lebitasy, J.-D. Hecq, J. Cadrobbi, D. Vanbeckbergen, J. Jamart, *Can J Hosp Pharm* **2009**, *62*, 34. b) S. Walker, F. Charbonneau, S. Law, *Can J Hosp Pharm* **2007**, *60*, 231. c) D. M. Hoffman, D. D. Grossano, L. Damin, T. M. Woodcock, *Am J Health Syst Pharm* **1979**, *36*, 1536.
[12] FDA, https://www.fda.gov/regulatory-information/search-fda-guidance-documents/q3c-tables-and-list-rev-4, accessed.
[13] C. Settembre, A. Ballabio, *Trends Cell Biol.* **2014**, *24*, 743.
[14] K. Sato, *Chem. Eng. Sci.* **2001**, *56*, 2255.
[15] a) K. F. Mück, O. Christ, H. M. Kellner, *Makromol. Chem.* **1977**, *178*, 2785; b) I. W. Davidson, H. S. Miller Jr, F. J. Dicarlo, *J. Pharm. Sci.* **1971**, *60*, 274; c) C. Peters, M. Hoop, S. Pané, B. J. Nelson, C. Hierold, *Adv. Mater.* **2016**, *28*, 533.
[16] N. Malekjani, S. M. Jafari, *Compr Rev Food Sci Food Saf* **2021**, *20*, 3.
[17] a) Y. Wang, G. Boero, X. Zhang, J. Brugger, *Adv. Mater. Interfaces* **2020**, *7*, 2000733; b) R. R. Shah, T. P. Davis, A. L. Glover, D. E. Nikles, C. S. Brazel, *J. Magn. Magn. Mater.* **2015**, *387*, 96.
[18] a) L. F. Fajardo LG, *Cancer Res.* **1984**, *44*, 4826s; b) J. Van der Zee, *Ann. Oncol.* **2002**, *13*, 1173.
[19] M. Caine, S. Bian, Y. Tang, P. Garcia, A. Henman, M. Dreher, D. Daly, R. Carlisle, E. Stride, S. L. Willis, *Eur. J. Pharm. Sci.* **2021**, *160*, 105772.